DMD Fast Forward. Published on October 5, 2020 as DOI: 10.1124/dmd.120.000098
This article has not been copyedited and formatted. The final version may differ from this version.

1. Title Page

Title

A multi compartment human kidney proximal tubule-on-a-chip replicates cell polarization-dependent cisplatin toxicity[a,b,c,d]

Authors

Tom T.G. Nieskens[1], Mikael Persson[1], Edward J. Kelly[2,3] and Anna-Karin Sjögren[1]

Primary laboratory of origin

CVRM Safety, Clinical Pharmacology and Safety Sciences, R&D, AstraZeneca, Gothenburg, Sweden

Affiliations

TTGN, MP, AKS: CVRM Safety, Clinical Pharmacology and Safety Sciences, R&D, AstraZeneca, Gothenburg, Sweden

EJK: Department of Pharmaceutics, University of Washington, Seattle, USA

EJK: Kidney Research Institute, University of Washington, Seattle, USA

DMD Fast Forward. Published on October 5, 2020 as DOI: 10.1124/dmd.120.000098
This article has not been copyedited and formatted. The final version may differ from this version.

2. Running Title Page

Running title

Polarization determines kidney-on-a-chip cisplatin toxicity

Corresponding author

Anna-Karin Sjögren

AstraZeneca R&D Mölndal

Pepparedsleden 1

43150 Mölndal

Sweden

anna-karin.sjogren@astrazeneca.com

Number of text pages: 16

Number of tables: 1

Number of figures: 5

Number of references: 56

Number of words in the Abstract: 249

Number of words in the Introduction: 669

Number of words in the Discussion: 1484

Nonstandard abbreviations

2D: 2-dimensional

3D: 3-dimensional

AKI: acute kidney injury

AQP1: aquaporin 1

BCRP: breast cancer resistance protein

BSA: bovine serum albumin

DMD Fast Forward. Published on October 5, 2020 as DOI: 10.1124/dmd.120.000098
This article has not been copyedited and formatted. The final version may differ from this version.

CTR1: high affinity copper uptake protein 1

DCC: dual channel chip

DIKI: drug-induced kidney injury

DPBS: Dulbecco's phosphate buffered saline

FCS: fetal calf serum

HBSS: Hank's balanced salt solution

HRPTEC: human-derived renal proximal tubule epithelial cells

LDH: lactate dehydrogenase

LLC-PK1: Lilly Laboratories Cell-Porcine Kidney 1

MATE1: multidrug and toxin extrusion transporter 1

MATE2-k: multidrug and toxin extrusion transporter 2-k

MPS: microphysiological systems

Na^+/K^+-ATPase: sodium-potassium adenosine triphosphatase

Nrf2: nuclear factor erythroid 2-related factor 2

OCT2: organic cation transporter 2

P-gp: P-glycoprotein

PDMS: polydimethylsiloxane

PTEC: proximal tubule epithelial cells

RVK: reservoir kit

ZO-1: zona occludens-1

DMD Fast Forward. Published on October 5, 2020 as DOI: 10.1124/dmd.120.000098
This article has not been copyedited and formatted. The final version may differ from this version.

3. Abstract

Drug-induced kidney injury (DIKI) is a major clinical problem and causes drug attrition in the pharmaceutical industry. To better predict DIKI, kidney *in vitro* cultures with enhanced physiological relevance are developed. To mimic the proximal tubule, the main site of adverse drug reactions in the kidney, human-derived renal proximal tubule epithelial cells (HRPTEC) were injected in one of the channels of dual channel Nortis® chips and perfused for 7 days. Tubes of HRPTEC demonstrated expression of tight junction protein 1 (ZO-1), lotus lectin and primary cilia, with localization at the apical membrane, indicating an intact proximal tubule brush border. Gene expression of cisplatin efflux transporters MATE1 (*SLC47A1*) and MATE2-k (*SLC47A2*), and Megalin endocytosis receptor (*LRP2*) increased 19.9±5.0, 23.2±8.4 and 106±33-fold, respectively, in chip cultures compared to 2D cultures. Moreover, organic cation transporter 2 (OCT2, *SLC22A2*) was localized exclusively on the basolateral membrane. When infused from the basolateral compartment, cisplatin (25 µM, 72 h) induced toxicity, evident as reduced cell number and reduced barrier integrity compared to vehicle-treated chip cultures. Co-exposure with the OCT2 inhibitor cimetidine (1 mM) abolished cisplatin toxicity. In contrast, infusion of cisplatin from the apical compartment did not induce toxicity, in line with polarized localization of cisplatin uptake transport proteins, including OCT2. In conclusion, we developed a dual channel human kidney proximal tubule-on-a-chip with a polarized epithelium, restricting cisplatin sensitivity to the basolateral membrane, suggesting improved physiological relevance over single compartment models. Its implementation in drug discovery holds promise to improve future *in vitro* DIKI studies.

DMD Fast Forward. Published on October 5, 2020 as DOI: 10.1124/dmd.120.000098
This article has not been copyedited and formatted. The final version may differ from this version.

4. Significance Statement

Human-derived kidney proximal tubule cells retained characteristics of epithelial polarization *in vitro* when cultured in the kidney-on-a-chip, and the dual channel construction allowed for drug exposure using the physiologically-relevant compartment. Therefore, cell polarization-dependent cisplatin toxicity could be replicated for the first time in a kidney proximal tubule-on-a-chip. The use of this physiological relevant model in drug discovery has potential to aid identification of safe novel drugs and contribute to reducing attrition rates due to drug-induced kidney injury.

DMD Fast Forward. Published on October 5, 2020 as DOI: 10.1124/dmd.120.000098
This article has not been copyedited and formatted. The final version may differ from this version.

5. Introduction

The proximal tubule epithelium is the tissue within the kidney that is most prone to drug-related adverse effects. Renal proximal tubule epithelial cells (RPTEC) are tasked with the active excretion of waste products, including urea and uremic toxins, and reabsorption of essential molecules, including water, salts, glucose, amino acids and proteins (Nigam et al., 2015). To this end, RPTEC express specialized transmembrane drug transporter proteins, facilitating influx from the kidney interstitium and efflux to the glomerular filtrate, collectively referred to as transcellular transport, clearing compounds from the internal circulation. Imbalances between influx and efflux however, can render RPTEC vulnerable to drug-induced toxicity (Konig et al., 2013; Nigam et al., 2015; Nieskens and Sjogren, 2019).

The main adverse effect of the chemotherapeutic cisplatin is acute kidney injury (AKI), which occurs in approximately 30% of patients (Hartmann et al., 1999). Cisplatin is taken up by organic cation transporter 2 (OCT2, *SLC22A2*) located on the basolateral membrane of RPTEC (Ciarimboli et al., 2005; Yonezawa et al., 2005; Filipski et al., 2008; Ciarimboli et al., 2010) and excreted by multidrug and toxin extrusion transporter 1 (MATE1, *SLC47A1*) and, to a lesser extent, multidrug and toxin extrusion transporter 2-k (MATE2-k, *SLC47A2*) located on the apical membrane of RPTEC (Yonezawa et al., 2006; Nakamura et al., 2010; Li et al., 2013). The toxic potential of cisplatin correlates directly to its accumulation, which is in turn determined by the activity of cation influx and efflux transporters (Li et al., 2013). The physiological relevance and predictive value of *in vitro* proximal tubule models for nephrotoxic drugs is therefore in part dependent on the ability to form distinct apical and basolateral membranes, referred to as polarization, which enables epithelial barrier formation and correct membrane localization of drug transporters similar to *in vivo* (Ito et al., 2005; Stoops and Caplan, 2014).

Kidney *in vitro* models are valuable tools for preclinical investigation of drug-induced toxicity, but inherently suffer from partial dedifferentiation (Lash et al., 2006; Brown et al., 2008; Lash et al., 2008). This reduces tight junction expression and epithelial barrier function, and limits replication of cell polarization-dependent drug-induced toxicity (Lash et al., 2018). By recapitulating the microenvironment of the physiological proximal tubule, recently developed kidney-on-a-chip models, also known as kidney microphysiological

DMD Fast Forward. Published on October 5, 2020 as DOI: 10.1124/dmd.120.000098
This article has not been copyedited and formatted. The final version may differ from this version.

systems (MPS), aim to enhance proximal tubule cultures towards their *in vivo* phenotype (Jang et al., 2013; Weber et al., 2016; Vedula et al., 2017; Vriend et al., 2018). Epithelial polarization has been confirmed in these chip systems by tight junction formation and the presence of primary cilia (Jang et al., 2013; Jansen et al., 2015; Weber et al., 2016; Vedula et al., 2017; Vormann et al., 2018; Vriend et al., 2018), as well as proof-of-concept studies indicating that transepithelial transport of anionic and cationic organic compounds is feasible (Weber et al., 2016; Jansen et al., 2019; van der Made et al., 2019; Stahl et al., 2020). Kidney-on-a-chip models have been used to study drug-induced toxicity (Jang et al., 2013; Sakolish et al., 2018; Suter-Dick et al., 2018; Weber et al., 2018; Vormann et al., 2018; Maass et al., 2019), but crucially have not previously been applied to study the implications of epithelial polarization and localization of drug transporters for replication of membrane-dependent drug toxicity *in vitro*.

The aim of this study was to develop a human-derived kidney proximal tubule-on-a-chip that is capable of replicating polarization-dependent nephrotoxicity, using cisplatin as model compound. Polarization of the proximal tubule epithelium was demonstrated by apical localization of tight junctions and primary cilia, and basolateral localization of OCT2. Moreover, correct polarized localization and function of cisplatin influx transporters was confirmed when toxicity induced by cisplatin was only observed if perfused from the basolateral compartment and not when perfused from the apical compartment. Polarization is crucial for the physiological relevance of an *in vitro* model and, when implemented at a fitting stage of drug discovery, this kidney-on-a-chip has the potential to aid the selection of drugs with the right safety profile, improve safety translation and contribute to bringing safer drugs to the patients.

DMD Fast Forward. Published on October 5, 2020 as DOI: 10.1124/dmd.120.000098
This article has not been copyedited and formatted. The final version may differ from this version.

6. Materials and Methods

Cell culture

Cryopreserved human-derived renal proximal tubule epithelial cells (HRPTEC, batch RPT101030, male, mycoplasma negative) were purchased from Biopredic (Rennes, France). To increase homogeneity, cells of passage 2 were expanded once in T75 Nunc culture flasks (Thermo Fisher, Waltham, USA), before seeding in either 12-well plates or 96-well plates (Corning Life Sciences, Corning, New York) with a density of 75,000 cells/cm^2 for regular monolayer cultures. In the microphysiological chips (Nortis, Inc., Seattle, USA), cells were seeded at $10x10^6$ cells/ml. Cells were incubated at 37°C and 5% v/v CO_2 for 7 days before experimental intervention. Cells were cultured in Dulbecco's modified eagle medium/HAM's F12 with GlutaMAX™ supplement (Life Technologies, Paisley, UK), supplemented with 10 mg/ml insulin, 10 mg/ml transferrin, 10 mg/ml selenium, 24 ng/ml hydrocortisone, 10 ng/ml epidermal growth factor, 4 pg/ml tri-iodothyronine (Sigma, St. Louis, USA), 1% fetal calf serum (FCS; Life Technologies) and 1% penicillin/streptomycin (Life Technologies), the latter only during seeding. For regular culture plates, the medium was refreshed every 2 to 3 days, while medium is continuously perfused in the microphysiological chips at a rate of 1 µl/min.

Microphysiological chip preparation

Dual channel microphysiological chips (DCC-001), reservoir kits (RVK-001) and all other perfusion equipment was obtained from Nortis, Inc. (Woodinville, WA, USA) and handled according to the manufacturer's instructions. Briefly, the matrix compartment of each chip was first washed with 3 ml ethanol (99.5%; CCS Healthcare, Borlänge, Sweden) and dried by aspiration for 1.5 minutes. Next, rat tail-derived collagen I (7 mg/ml; Corning Life Sciences) was freshly supplemented with DPBS (1x), phenol red (0.004 mg/ml), HEPES (25 mM) and genipin (0.2 mM); final concentrations listed. Finally, NaOH and filter-sterilized deionised water were added to obtain a pH of 8.0-8.5. The matrix was subsequently injected into the matrix compartment of each chip, incubated at 4°C for 1-2 h, followed by overnight incubation at 37°C for polymerization. The two aligning fiber pins were removed from the chips the next day to form the tubular collagen lumen, both connecting their respective prefabricated

DMD Fast Forward. Published on October 5, 2020 as DOI: 10.1124/dmd.120.000098
This article has not been copyedited and formatted. The final version may differ from this version.

polydimethylsiloxane (PDMS) circuits. The circuits were perfused overnight with culture medium using the Nortis® pump setup at 1 µl/min. The next day, only one channel was injected (2x 2.5 µl) with freshly prepared collagen IV (10 µg/ml, Sigma) solution in DPBS (1x), to allow for coating of the lumen, and incubated at 37°C and 5% v/v CO_2. After 1 h, a suspension of cryopreserved HRPTEC in culture medium was injected (2x 2.5 µl) into the collagen IV coated channel at a density of $10x10^6$ cells/ml, and subsequently incubated at 37°C and 5% v/v CO_2. The matrix ports were closed after 4 h to prevent drying. Perfusion of both circuits was reinstated following overnight incubation, enabling the remaining, unattached cells to flush from the lumen. Medium was continuously perfused through both circuits in the microphysiological chips at a rate of 1 µl/min (fluid shear stress of 0.9 dyne/cm^2) for 7 days, allowing the cells to form a confluent tube-shaped monolayer.

Compound exposure, cell count, immunofluorescence staining and barrier integrity evaluation

In preparation for compound exposure in microphysiological chips, medium of the apical channel inflow reservoirs was supplemented with dextran 3000-Alexa Fluor 680 (0.02 mg/ml, Life Technologies). After 1 day, the outflow reservoirs of both the apical channels and basolateral channels were sampled for baseline values. Next, the medium in the apical channel or basolateral channel inflow reservoirs was replaced by medium containing cisplatin (25 µM, Sigma), with or without cimetidine (1 mM, Sigma), depending on the experimental condition. Outflow reservoirs of both channels were sampled at 24, 48 and 72 h. After 72h exposure, nuclear stain was performed by disconnecting chips from the perfusion system and perfused with HBSS (1x, 37°C) supplemented with Hoechst 33342 (1:1000, Life Technologies) at 1 µl/min for 2.5 h. Benchtop perfusions were performed at room temperature, using 5-ml syringes (Henke Sass Wolff, Tuttlingen, Germany) and CMA400 syringe pump (CMA Microdialysis, Kista, Sweden). Chips were imaged immediately at preset excitation and emission wavelengths (Table S1) at 20x magnification using ImageXpress Micro Confocal High-Content Imaging System (Molecular Devices, San Jose, USA). The same exposure times were used to establish a baseline in control chips and applied to treatment groups equally. After imaging, chips were treated further for immunofluorescence staining. Counting of nuclei was performed on a single representative section and single z-slice focused on the bottom of each tube, using ‘find maxima’ in Fiji (version 2.0.0) and a noise tolerance of 600 or 2500 for Hoechst 33342

DMD Fast Forward. Published on October 5, 2020 as DOI: 10.1124/dmd.120.000098
This article has not been copyedited and formatted. The final version may differ from this version.

(depending on the background). Values were expressed as percentage of vehicle and results were plotted with GraphPad Prism (version 8.01; GraphPad Software). Fluorescence intensity of labelled dextran was evaluated at excitation and emission wavelengths of 670 nm and 720 nm, respectively, using the Clariostar microplate reader (BMG Labtech, Ortenberg, Germany). Values were expressed as fold change compared to baseline and results were plotted with GraphPad Prism (version 8.01; GraphPad Software).

For immunofluorescence staining, chips were disconnected from the perfusion system and first perfused with HBSS (1x, 37°C) at 1 µl/min for 2.5 h. Next, chips were perfused with formaldehyde (4%, VWR, Spånga, Sweden) at 1 µl/min for 1.5 h, followed by wash buffer at 10 µl/min for 1 h. Wash buffer consisted of bovine serum albumin (2%, Sigma) and Triton X100 (1%, Sigma) in HBSS. Primary antibody was diluted to the indicated ratio in wash buffer (Table S1), and subsequently manually injected (200 µl) into the chips, followed by overnight incubation at 4°C. Next day, chips were first perfused with wash buffer at 10 µl/min for 1 h, followed by manual injection (200 µl) of secondary antibody (Table S1), supplemented with Hoechst 33342 (1:1000, Life Technologies) and optionally phalloidin-Alexa Fluor 647 (1:100, Life Technologies). The chips were perfused with wash buffer at 10 µl/min for 1 h, before imaging at preset excitation and emission wavelengths (Table S1) at 20x magnification, using ImageXpress Micro Confocal High-Content Imaging System (Molecular Devices). The intensity profile of the images was automatically rescaled to correct for background for visualization only and image montages were made using Fiji (version 2.0.0). For 3D reconstruction of tight junctions, the spinning disk confocal function (60 µm pinhole) was enabled before images were taken every 2 µm over 120 µm in the z-direction. Reconstruction was performed using ‘3D Project’ in Fiji, with ‘brightest point method’, 2 µm spacing between images and turning the resulting tube to an angle of 30°.

Gene expression analysis

For gene expression analysis in microphysiological chips, chips were disconnected from the perfusion system and first perfused with HBSS (1x, 37°C) at 1 µl/min for 2.5 h. Next, chips were perfused with RLT lysis buffer (Qiagen, Hilden, Germany) at 5 µl/min for 30 min and the perfusate was collected. After a static incubation for 30 min, chips were perfused again with RLT lysis buffer (Qiagen) at 5 µl/min for 40

DMD Fast Forward. Published on October 5, 2020 as DOI: 10.1124/dmd.120.000098
This article has not been copyedited and formatted. The final version may differ from this version.

min, collecting the perfusate. For gene expression analysis in regular monolayer cultures, cells seeded in 12-well plates were first washed 3x with HBSS (1x) and directly lysed in RLT lysis buffer (0.5 ml/well, Qiagen). RNA was isolated using the RNeasy Mini kit (Qiagen) according to the instructions as provided by the manufacturer. High Capacity cDNA Reverse transcription kit (Applied Biosystems, Foster City, USA) was used to synthesize cDNA at a final concentration of 6 ng/µl, according to the instructions as provided by the manufacturer. Expression levels of mRNA were determined using gene-specific primer probe sets (Table S2) and Taqman Fast Advanced Master Mix (Applied Biosystems) using the QuantStudio Flex 7 (Applied Biosystems) at a final concentration of 1.8 ng/µl cDNA and analyzed using Quantstudio Real Time PCR Software (version 1.3, Applied Biosystems). Expression levels in the microphysiological chips were expressed as $-\Delta\Delta C_t$ compared to regular monolayer cultures, using *GAPDH* as reference gene. Results were plotted with GraphPad Prism (version 8.01; GraphPad Software).

Transcellular 4-di-1-ASP transport assay

To evaluate transcellular transport capability of cations in microphysiological chips, chips were disconnected from the perfusion system and first perfused with HBSS (1x, 37°C) supplemented with HEPES (10 mM, Life Technologies) at 1 µl/min for 3 h. Next, perfusion of the basolateral channel was switched to HBSS-HEPES containing 4-di-1-ASP (100 µM, Life Technologies), with or without cimetidine (1 mM, Sigma), at 2 µl/min. The apical channel was perfused with HBSS-HEPES. Accumulative perfusate samples were collected from 6 h after initiation of perfusion for 14 h. Finally, 100 µl of each sample was transferred to a 96 well plate and fluorescence intensity of 4-di-1-ASP was evaluated at excitation and emission wavelengths of 485 nm and 590 nm, respectively, and a gain of 1600 using the Clariostar microplate reader (BMG Labtech). Values were expressed as arbitrary units, or blank subtracted and normalized against uninhibited control. Results were plotted with GraphPad Prism (version 8.01; GraphPad Software).

LDH evaluation

DMD Fast Forward. Published on October 5, 2020 as DOI: 10.1124/dmd.120.000098
This article has not been copyedited and formatted. The final version may differ from this version.

Lactate dehydrogenase (LDH), as measure for cell membrane integrity in regular 2D cultures, was evaluated from supernatant (10 µl) using the Pierce LDH Cytotoxicity Assay Kit (Thermo Fisher) according to the instructions as provided by the manufacturer. Reactions were run for 30 min and absorbance was evaluated at 490 nm and 680 nm using the Clariostar microplate reader (BMG Labtech). Values at 680 mn were subtracted from 490 nm and results were plotted with GraphPad Prism (version 8.01; GraphPad Software).

Cisplatin exposure measurements

To estimate the concentration chip-cultured cells are exposed to when cisplatin is perfused from the basolateral and apical compartments, chips were prepared as described earlier, while omitting cell injection to eliminate any drug-transporter or metabolic related effects. Basolateral exposure was evaluated by perfusing one channel with cisplatin (25 µM, Sigma) and the other with medium, collecting perfusate from the medium channels. Apical exposure was evaluated by perfusing only one channel with cisplatin (25 µM, Sigma) and collecting from the same, while the parallel channel is not perfused. Perfusions were performed using the Nortis® pump setup at 1 µl/min and samples were taken every 12 h for 72 h. Samples were processed first by passing them through a Microcon 30kDa microcentrifuge filter unit (Ultracel-30 membrane, Merck-Millipore, Burlington, MA, USA) using centrifugation for 10 min at 16000G and 4°C, filtrate (20 µl), diluted with internal standard (IS), and derivatized with diethylthiocarbamate (5% DDTC in sodium hydroxide solution, Sigma). Samples were diluted with acetonitrile/water (1/1 v/v) and cisplatin content was evaluated by UPLC MS/MS. Separation of derivatized cisplatin was achieved using UPLC with an Acquity BEH C18 column (Waters, Milford, MA, USA) and acetontirile/acetic acid (100/0.2 v/v) and ammonium formate (20 mM) mobile phase run under gradient conditions. Detection was via an API5000 mass spectrometer (Sciex, Framingham, MA, USA) in positive TurboIonSpray mode and results were plotted with GraphPad Prism (version 8.01; GraphPad Software).

Statistical analysis

All data analysis and statistics were performed using GraphPad Prism (version 8.01; GraphPad Software) and presented as mean±S.D. of three independent experiments (n=3) set in advance, unless stated

DMD Fast Forward. Published on October 5, 2020 as DOI: 10.1124/dmd.120.000098
This article has not been copyedited and formatted. The final version may differ from this version.

otherwise. The number of experimental replicates and total comparisons is indicated in the figure legends. Statistics were performed by (paired) Student's t tests (two-tailed, a=0.05), corrected for multiple comparisons using the Holm-Sidak method, one- or two-way ANOVA with Dunnett's multiple comparisons test ($P<0.05$), using multiplicity adjusted P-values.

DMD Fast Forward. Published on October 5, 2020 as DOI: 10.1124/dmd.120.000098
This article has not been copyedited and formatted. The final version may differ from this version.

7. Results

HRPTEC cultured in the kidney proximal tubule-on-a-chip were polarized with tight junctions and primary cilia localized on the apical brush border and OCT2 strictly localized on the basolateral membrane

To increase the physiological relevance of the culture environment, HRPTEC were cultured in Nortis® dual channel microphysiological chips. These consist of two parallel collagen IV-coated hollow channels inside a larger compound-permeable collagen I matrix, that allows for independent medium perfusion through separate channel circuits (Figure 1A). When HRPTEC were injected into a single channel and perfused with culture medium at 1 µl/min (fluid shear stress of 0.9 dyne/cm^2), cells attached directly to collagen IV and 3-dimensional (3D) tube formation was observed over the course of 7 days (Figure 1B). The remaining empty channel was also perfused, generating a culture system with distinct apical and basolateral compartments, representing the tubule lumen and the kidney interstitium, respectively. To investigate cellular polarization, HRPTEC were subsequently stained with antibodies for confocal fluorescence imaging at the positions indicated in Figure 1E. Tubes demonstrated a characteristic epithelial expression pattern of tight junction protein, highlighting cell-cell interactions, with focused expression at the apical membrane (Figure 1C). A 3D reconstruction of the tight junction pattern using confocal imaging confirmed an elongated, tube-shaped tissue structure (Figure 1D). In addition, tubes showed apical localization of lotus lectin (LTL), the presence of primary cilia protruding from the apical membrane into the tubule lumen (by staining for acetylated alpha tubulin), and strict basolateral localization of OCT2 (Figure 1C), together demonstrating an intact tubule brush border that is tight and polarized. Finally, phalloidin was used to demonstrate that F-actin is mainly located at the cell borders and the basolateral membrane, which is a typical distribution for epithelial cells (Figure 1C).

Gene expression of MATE1 and MATE2-k efflux drug transporters increased in HRPTEC cultured in the kidney proximal tubule-on-a-chip compared to regular 2D cultures

Next, gene expression of several drug transporters and proximal tubule markers in chip-cultured HRPTEC was compared to regular 2-dimensional (2D) HRPTEC cultures (Figure 2, Table 1). Expression of MATE1

DMD Fast Forward. Published on October 5, 2020 as DOI: 10.1124/dmd.120.000098
This article has not been copyedited and formatted. The final version may differ from this version.

(*SLC47A1*) and MATE2-k (*SLC47A2*), both responsible for cisplatin efflux, increased 19.9±5.0 and 23.2±8.4-fold (mean±S.D., n=5), respectively, when HRTPEC were cultured in the chips compared to regular 2D cultures (Figure 2, Table 1). Cisplatin uptake transporters OCT2 (*SLC22A2*) and high affinity copper uptake transporter 1 (CTR1, *SLC31A1*) were expressed at similar levels in chip-cultured and regular 2D cultured HRPTEC (Figure 2, Table 1). In addition, chip-cultured HRPTEC increased expression of Megalin endocytosis receptor (*LRP2*) with 106±33-fold (mean±S.D., n=5) and expression of efflux transporter breast cancer resistance protein (BCRP, *ABCG2*) with 4.3±0.4-fold (mean±S.D., n=3), while the expression of efflux transporter P-glycoprotein (P-gp, *ABCB1*) was decreased to 0.32±0.06-fold (mean±S.D., n=5) (Figure 2, Table 1). Interestingly, organic anion transporter 1 (OAT1, *SLC22A6)* was expressed exclusively in chip-cultured HRPTEC (ΔC_t of 11.8±0.8 relative to *GAPDH*, n=5, Table 1) and was not detected in regular 2D cultures. Gene expression of organic anion transporter 3 (OAT3, *SLC22A8*) was, however, not detected in neither regular 2D or chip-cultured HRPTEC (Table 1).

A trend towards transepithelial transport of fluorescent organic cation 4-di-1-ASP was observed in the kidney proximal tubule-on-a-chip

To investigate the concerted activity of cation influx and efflux transport mechanisms in the human kidney proximal tubule-on-a-chip, transcellular transport of 4-di-1-ASP was evaluated. The fluorescent organic cation 4-di-1-ASP is reported to be a substrate for both OCT2 and MATE1/2-k drug transporters, covering the cation transcellular transport axis (Biermann et al., 2006; Wittwer et al., 2013). To this end, 4-di-1-ASP (100 µM) was perfused into the basolateral compartment while buffer was perfused into the apical compartment, so that fluorescence intensity of accumulative apical perfusate (14 h) reflects compound transfer (Figure 3A). As expected, the apical fluorescence signal was reduced compared to the basolateral signal as it reflects HRPTEC epithelial barrier integrity (Figure S1). The active transport component was evaluated by supplementing 4-di-1-ASP with competitive OCT2 inhibitor cimetidine (1 mM, Figure 3B). A trend towards cimetidine-mediated inhibition of 4-di-1-ASP transfer was observed in every individual experiment (66%, 30% and 17%; with an average of 38±25% (mean±S.D., n=3, Figure 3B)), but was not statistically significant (paired Student's t-test, P=0.18).

DMD Fast Forward. Published on October 5, 2020 as DOI: 10.1124/dmd.120.000098
This article has not been copyedited and formatted. The final version may differ from this version.

Cisplatin induced toxicity in the kidney proximal tubule-on-a-chip exclusively when exposed to the basolateral membrane and toxicity was abolished by the OCT2 inhibitor cimetidine

When HRPTEC were cultured in regular 96-well plates, cisplatin (12.5-50 µM) induced toxicity, as demonstrated by a time- and concentration-dependent increase of lactate dehydrogenase (LDH) in the supernatant (Figure S2). As expected, toxicity was attenuated by co-incubation with cimetidine (1 mM), indicating its dependence on OCT2 influx activity (Figure S2). In contrast to regular 2D cultures, the dual channel chip layout allows for selective exposure of the proximal tubule apical or basolateral membrane, which is relevant when mimicking physiological exposure to therapeutics *in vitro*. When cisplatin (25 µM) was perfused for 72 h from the basolateral channel, mimicking exposure through the clinically relevant interstitium and internal circulation, the tight junction pattern on the bottom slice of the tube was partly disrupted (Figure 4A) and cell count was reduced to 41.2±6.6% (mean±S.D., n=5) compared to vehicle control (Figure 4B). This resulted in a concomitant 8.7±6.3-fold (mean±S.D., n=4) increase in paracellular diffusion of dextran 3000 across the epithelium, from the apical into the basolateral compartment (Figure 4C). As expected, co-incubation with the OCT2-inhibitor cimetidine (1 mM) abolished all toxic effects, demonstrating that cisplatin-induced toxicity is dependent on OCT2 influx activity (Figure 4 A-C). The actual concentration of cisplatin reaching the cells through basolateral exposure was measured by omitting cell injections, perfusing the basolateral channel with cisplatin (25 µM) and collecting the perfusate from the apical channel (Figure 5A). The resulting concentration of cisplatin was 3.4±0.05 µM (at 24 h, mean±S.D., n=3, Figure 5C), which is similar to clinical therapeutic total plasma concentrations reported in literature, although this is dependent on the dosing regimen applied (Himmelstein et al., 1981; Ikeda et al., 1998; Petrillo et al., 2019). In contrast, when cisplatin was perfused from the apical channel, mimicking exposure through the tubule lumen, toxicity was not observed (Figure 4 A-C). The concentration of cisplatin through apical exposure was evaluated by perfusing the apical channel with cisplatin (25 µM) and collecting perfusate from the apical channel (Figure 5B), resulting in an actual exposure of 20.2±1.3 µM (at 24 h, mean±S.D., n=3, Figure 5C). So, even though apical cisplatin exposure was more than 5-fold higher than the basolateral exposure, it did not induce toxicity. These results confirm that the transporters meditating cisplatin toxicity were uniquely expressed on the basolateral membrane, supporting the epithelial polarization of this proximal tubule-on-a-chip.

DMD Fast Forward. Published on October 5, 2020 as DOI: 10.1124/dmd.120.000098
This article has not been copyedited and formatted. The final version may differ from this version.

DMD Fast Forward. Published on October 5, 2020 as DOI: 10.1124/dmd.120.000098
This article has not been copyedited and formatted. The final version may differ from this version.

8. Discussion

Achieving a safety profile for candidate drugs lacking renal adverse effects prior to the clinical phase of development, requires predictive and physiologically relevant *in vitro* proximal tubule epithelial models. Here, we developed a human-derived kidney proximal tubule-on-a-chip that demonstrates epithelial polarization with intact tight junctions and primary cilia on the apical brush border membrane and strict localization of OCT2 on the basolateral membrane. Exclusive OCT2-dependent sensitivity to the nephrotoxic drug cisplatin was shown when the tube is exposed via the basolateral compartment, while toxicity was not observed when exposed to more than 5-fold higher concentration via the apical compartment. Therefore, the importance of polarized localization of cation drug uptake transporters to more accurately replicate drug-induced kidney toxicity was demonstrated for the first time in a chip-based proximal tubule model.

Influx of cisplatin into renal proximal tubule epithelial cells and the nephrotoxicity this results in, has been shown to be mediated by OCT2 (Ciarimboli et al., 2005; Yonezawa et al., 2005; Yonezawa et al., 2006; Ciarimboli et al., 2010) and high affinity copper uptake protein 1 (CTR1, *SLC31A1*) (Pabla et al., 2009). OCT2 is a facilitated diffusion transporter driving the influx of cationic compounds across the basolateral membrane using the inward-directed negative membrane potential (Okuda et al., 1999b; Budiman et al., 2000). The current study showed attenuation of cisplatin toxicity by cimetidine in both regular 2D HRPTEC cultures and chip-cultured HRPTEC, demonstrating OCT2 activity is the main contributing factor to cisplatin toxicity and confirming previous results *in vitro* (Yonezawa et al., 2005; Yonezawa et al., 2006; Sato et al., 2008) and *in vivo* (Ciarimboli et al., 2010; Katsuda et al., 2010). It is worth noticing however, that the cimetidine concentration used is higher than a typical pharmacological concentration, as the C_{max} is reported to be 16 µM (Schmidt et al., 1998). Moreover, the current study elegantly demonstrates that when HRPTEC cultures are correctly polarized, form tight junctions and concentrate OCT2 strictly on the basolateral membrane, cisplatin only induced toxicity when the basolateral membrane is exposed, and at clinically relevant total plasma concentrations (Himmelstein et al., 1981; Ikeda et al., 1998; Petrillo et al., 2019). While the toxicity data presented in the current manuscript support OCT2-mediated cisplatin transport, future intracellular accumulation and transcellular transport studies using cisplatin as substrate

DMD Fast Forward. Published on October 5, 2020 as DOI: 10.1124/dmd.120.000098
This article has not been copyedited and formatted. The final version may differ from this version.

may provide further insights into actual handling of this nephrotoxicant by the proximal tubule-on-a-chip. Cisplatin toxicity has previously been evaluated in a few chip-based models. Jang et al. (2013) showed that cisplatin exposed basolaterally induced toxicity in their 2D chip-based model but the concentration used (100 µM) extends beyond the therapeutic concentration and cellular cisplatin exposure was not evaluated (Himmelstein et al., 1981; Jang et al., 2013). In other studies, both compartments were used simultaneously, which prohibited any evaluation of the impact of epithelial polarization on cisplatin sensitivity (Suter-Dick et al., 2018; Vormann et al., 2018). In contrast to the current study, single channel Nortis® proximal tubule-on-a-chips were used to show that apical cisplatin exposure (1 µM) increased concentrations of Kidney Injury Molecule-1 (KIM1) in the supernatant, while LDH levels (reflecting cytotoxicity) were not affected (Sakolish et al., 2018; Maass et al., 2019). While we can only speculate about the reason for the discrepancy compared to the current study, it may be explained by differences in exposure times and endpoints used, assays, cell source and media components. An earlier study employing Lilly Laboratories Cell-Porcine Kidney 1 (LLC-PK_1) cells cultured on porous membrane inserts, showed that basolateral treatment with cisplatin (300 µM) induced a higher degree of cytotoxicity compared to apical treatment, confirming the current findings, although the applied concentration is not regarded as clinically relevant and localization of OCT2 was not investigated (Okuda et al., 1999a).

In contrast to the cisplatin parent compound, proximal tubule uptake of its metabolites is suggested to be mediated through alternative mechanisms (Townsend et al., 2009). Extrarenal glutathione conjugation generates water-soluble molecules, capable of being filtered by the glomerulus, therefore mainly exposing the apical membrane of proximal tubule cells. Interestingly, inhibition of γ-glutamyl transpeptidase or systeine s-conjugate β-lyase, vital enzymes in the conjugation pathway, or shifting the equilibrium towards oxidized glutathione, can both reduce proximal tubule toxicity in mice, indicating that cisplatin-glutathione contributes to nephrotoxicity, even when exposure is predominantly apical (Townsend and Hanigan, 2002; Jenderny et al., 2010). Extrarenal metabolite formation is not incorporated in the proximal tubule-on-a-chip described in the current study. However, it could be extended with a liver-on-a-chip compartment, making it suitable to study the contribution of metabolites to drug-induced nephrotoxicity, as shown earlier for ifosfamide and aristolochic acid (Choucha-Snouber et al., 2013; Chang et al., 2017).

DMD Fast Forward. Published on October 5, 2020 as DOI: 10.1124/dmd.120.000098
This article has not been copyedited and formatted. The final version may differ from this version.

Cisplatin efflux from the proximal tubule is mainly mediated by MATE1 (Yonezawa et al., 2006; Nakamura et al., 2010; Li et al., 2013). The current study showed significantly increased gene expression of MATE1 and MATE2-k in chip-cultured HRPTEC compared to regular 2D cultures, which suggests a more physiologically relevant phenotype. However, immunofluorescence did not succeed to detect specific staining of MATE1 or MATE2-k in the proximal tubule-on-a-chip (data not shown), most likely due to poor specificity of the primary antibodies, requiring extended optimization. Therefore, localization of these transporters remains to be elucidated in future studies. Treating HPRTEC with bardoxolone methyl, an inducer of signaling by the nuclear factor erythroid 2-related factor 2 (Nrf2) pathway, increases MATE1 gene expression and reduces cisplatin sensitivity (Atilano-Roque et al., 2016). Interestingly, Nrf2 has also been shown to regulate MATE2-K in response to flow in proximal tubule cells (Fukuda et al., 2017), sparking speculation that Nrf-signaling might explain upregulation of MATE gene expression observed in the current study.

Transepithelial transport activity is indicative of a polarized epithelial phenotype, as was previously shown for organic anions (Weber et al., 2016; Jansen et al., 2019; van der Made et al., 2019). The current study did not demonstrate a statistically significant inhibition of 4-di-1-ASP transepithelial transport using cimetidine, and therefore concerted activity of OCT2 and MATE1/2-k. However, the observed trend in inhibition is in line with the findings by Stahl et al. (2020), who demonstrated transcellular transport of cation drug metformin in a proximal tubule-on-a-chip using the same chip platform, although a different tissue donor was employed (Stahl et al., 2020). Differences in methods might explain this discrepancy, as radioactively labelled metformin was used as cation substrate combined with inhibitor imipramine, and this substrate and inhibitor combination reflects a different inhibition potential. In addition, increased sensitivity of detection due to radioactive labelling compared to the fluorescent methods used in the current study, potentially allows detection of inhibition across a wider range of substrate concentration (Stahl et al., 2020). In turn, variations in substrate transfer might reflect chip-to-chip differences in barrier integrity, increasing the diffusion component of substrate transfer across the epithelial tube, highlighting that advanced chip-based culture models remain technically challenging. MATE-mediated transport is driven

DMD Fast Forward. Published on October 5, 2020 as DOI: 10.1124/dmd.120.000098
This article has not been copyedited and formatted. The final version may differ from this version.

by a concentration gradient of H^+ over the brush border membrane (Tsuda et al., 2007; Sato et al., 2008; Konig et al., 2011). It has been shown that evaluation of cisplatin transport by MATE1 *in vitro* requires artificially acidifying the cytoplasm, reversing the naturally occurring H^+ gradient and direction of MATE1-mediated transport (Nakamura et al., 2010). Therefore, transepithelial transport activity and MATE-mediated efflux of cisplatin in chip-cultured HRPTEC may be investigated in future studies by increasing the acidity of the luminal chip channel, providing a more physiologically relevant driving force. In addition, genetic knockdown or knockout approaches would be a suitable future strategy to provide more direct evidence of OCT- and MATE-mediated transport function in the currently developed proximal tubule-on-a-chip.

The current study found significantly increased gene expression of *LRP2*, coding for the Megalin endocytosis receptor, in chip-cultured HRPEC compared to regular 2D HRPTEC cultures. Megalin is expressed on the apical brush border of proximal tubule cells and is responsible for reabsorption of low-molecular weight proteins and albumin from the glomerular filtrate (Nielsen et al., 2016). Increased uptake of Megalin substrate bovine serum albumin (BSA) has been described in response to changes in fluid flow (Ferrell et al., 2012; Jang et al., 2013; Raghavan et al., 2014; Ferrell et al., 2018). More recently, endocytosis activity has also been implicated in the uptake of antisense oligonucleotides (ASOs) into the proximal tubule epithelium (Janssen et al., 2019). Therefore, future studies may investigate whether the proximal tubule model developed here is suited to study ASO-induced renal adverse effects or the effects of fluid flow on receptor-mediated endocytosis.

In conclusion, the current study presented the first kidney proximal tubule-on-a-chip in which a nephrotoxic drug has been exposed through both the clinically relevant and non-relevant compartment, to demonstrate the contribution of epithelial polarization and membrane localization of drug influx mechanisms, in achieving drug sensitivity at clinically relevant concentrations. Therefore, the developed *in vitro* model displays increased physiological relevance compared to single-compartment models, and could be applied in the future to improve preclinical prediction of drug-induced kidney toxicity and eventually reduce kidney-related adverse effects of candidate drugs in the clinic.

DMD Fast Forward. Published on October 5, 2020 as DOI: 10.1124/dmd.120.000098
This article has not been copyedited and formatted. The final version may differ from this version.

DMD Fast Forward. Published on October 5, 2020 as DOI: 10.1124/dmd.120.000098
This article has not been copyedited and formatted. The final version may differ from this version.

9. Acknowledgements

The authors would like to thank Pedro Pinto and Simone Stahl for practical training and extended discussions on the experimental setup. Thanks to Magnus Söderberg for discussions on research design. Thanks to Glen Hawthorne for quantification of the cisplatin perfusion samples and to Sam Peel for providing imaging trays. Thanks to Otto Magnusson for contributing to the gene expression analysis. Special thanks to Marianna Stamou for expert help with imaging.

10. Authorship Contributions

Participated in research design: Nieskens, Kelly, Sjögren

Conducted experiments: Nieskens

Contributed new reagents or analytic tools: -

Performed data analysis: Nieskens, Sjögren

Wrote or contributed to the writing of the manuscript: Nieskens, Persson, Kelly, Sjögren

11. References

Atilano-Roque A, Aleksunes LM, and Joy MS (2016) Bardoxolone methyl modulates efflux transporter and detoxifying enzyme expression in cisplatin-induced kidney cell injury. *Toxicology letters* **259:**52-59.

Biermann J, Lang D, Gorboulev V, Koepsell H, Sindic A, Schröter R, Zvirbliene A, Pavenstädt H, Schlatter E, and Ciarimboli G (2006) Characterization of regulatory mechanisms and states of human organic cation transporter 2. *American journal of physiology Cell physiology* **290:**C1521-1531.

Brown CD, Sayer R, Windass AS, Haslam IS, De Broe ME, D'Haese PC, and Verhulst A (2008) Characterisation of human tubular cell monolayers as a model of proximal tubular xenobiotic handling. *Toxicology and applied pharmacology* **233:**428-438.

Budiman T, Bamberg E, Koepsell H, and Nagel G (2000) Mechanism of electrogenic cation transport by the cloned organic cation transporter 2 from rat. *The Journal of biological chemistry* **275:**29413-29420.

Chang SY, Weber EJ, Sidorenko VS, Chapron A, Yeung CK, Gao C, Mao Q, Shen D, Wang J, Rosenquist TA, Dickman KG, Neumann T, Grollman AP, Kelly EJ, Himmelfarb J, and Eaton DL (2017) Human liver-kidney model elucidates the mechanisms of aristolochic acid nephrotoxicity. *JCI insight* **2**.

Choucha-Snouber L, Aninat C, Grsicom L, Madalinski G, Brochot C, Poleni PE, Razan F, Guillouzo CG, Legallais C, Corlu A, and Leclerc E (2013) Investigation of ifosfamide nephrotoxicity induced in a liver-kidney co-culture biochip. *Biotechnology and bioengineering* **110:**597-608.

Ciarimboli G, Deuster D, Knief A, Sperling M, Holtkamp M, Edemir B, Pavenstadt H, Lanvers-Kaminsky C, am Zehnhoff-Dinnesen A, Schinkel AH, Koepsell H, Jurgens H, and Schlatter E (2010) Organic cation transporter 2 mediates cisplatin-induced oto- and nephrotoxicity and is a target for protective interventions. *The American journal of pathology* **176:**1169-1180.

Ciarimboli G, Ludwig T, Lang D, Pavenstadt H, Koepsell H, Piechota HJ, Haier J, Jaehde U, Zisowsky J, and Schlatter E (2005) Cisplatin nephrotoxicity is critically mediated via the human organic cation transporter 2. *The American journal of pathology* **167:**1477-1484.

Ferrell N, Cheng J, Miao S, Roy S, and Fissell WH (2018) Orbital Shear Stress Regulates Differentiation and Barrier Function of Primary Renal Tubular Epithelial Cells. *ASAIO journal (American Society for Artificial Internal Organs : 1992)* **64:**766-772.

Ferrell N, Ricci KB, Groszek J, Marmerstein JT, and Fissell WH (2012) Albumin handling by renal tubular epithelial cells in a microfluidic bioreactor. *Biotechnology and bioengineering* **109:**797-803.

Filipski KK, Loos WJ, Verweij J, and Sparreboom A (2008) Interaction of Cisplatin with the human organic cation transporter 2. *Clinical cancer research : an official journal of the American Association for Cancer Research* **14:**3875-3880.

Fukuda Y, Kaishima M, Ohnishi T, Tohyama K, Chisaki I, Nakayama Y, Ogasawara-Shimizu M, and Kawamata Y (2017) Fluid shear stress stimulates MATE2-K expression via Nrf2 pathway activation. *Biochemical and biophysical research communications* **484:**358-364.

Hartmann JT, Kollmannsberger C, Kanz L, and Bokemeyer C (1999) Platinum organ toxicity and possible prevention in patients with testicular cancer. *International journal of cancer* **83:**866-869.

Himmelstein KJ, Patton TF, Belt RJ, Taylor S, Repta AJ, and Sternson LA (1981) Clinical kinetics on intact cisplatin and some related species. *Clinical pharmacology and therapeutics* **29:**658-664.

Ikeda K, Terashima M, Kawamura H, Takiyama I, Koeda K, Takagane A, Sato N, Ishida K, Iwaya T, Maesawa C, Yoshinari H, and Saito K (1998) Pharmacokinetics of cisplatin in combined cisplatin and 5-fluorouracil therapy: a comparative study of three different schedules of cisplatin administration. *Japanese journal of clinical oncology* **28:**168-175.

Ito K, Suzuki H, Horie T, and Sugiyama Y (2005) Apical/basolateral surface expression of drug transporters and its role in vectorial drug transport. *Pharmaceutical research* **22:**1559-1577.

Jang KJ, Mehr AP, Hamilton GA, McPartlin LA, Chung S, Suh KY, and Ingber DE (2013) Human kidney proximal tubule-on-a-chip for drug transport and nephrotoxicity assessment. *Integrative biology : quantitative biosciences from nano to macro* **5:**1119-1129.

Jansen J, De Napoli IE, Fedecostante M, Schophuizen CM, Chevtchik NV, Wilmer MJ, van Asbeck AH, Croes HJ, Pertijs JC, Wetzels JF, Hilbrands LB, van den Heuvel LP, Hoenderop JG, Stamatialis D, and Masereeuw R (2015) Human proximal tubule epithelial cells cultured on hollow fibers: living membranes that actively transport organic cations. *Scientific reports* **5:**16702.

Jansen J, Jansen K, Neven E, Poesen R, Othman A, van Mil A, Sluijter J, Sastre Torano J, Zaal EA, Berkers CR, Esser D, Wichers HJ, van Ede K, van Duursen M, Burtey S, Verhaar MC, Meijers B, and Masereeuw R (2019) Remote sensing and signaling in kidney proximal tubules stimulates gut microbiome-derived organic anion secretion. *Proceedings of the National Academy of Sciences of the United States of America* **116:**16105-16110.

Janssen MJ, Nieskens TTG, Steevels TAM, Caetano-Pinto P, den Braanker D, Mulder M, Ponstein Y, Jones S, Masereeuw R, den Besten C, and Wilmer MJ (2019) Therapy with 2'-O-Me Phosphorothioate Antisense Oligonucleotides Causes Reversible Proteinuria by Inhibiting Renal Protein Reabsorption. *Molecular therapy Nucleic acids* **18:**298-307.

Jenderny S, Lin H, Garrett T, Tew KD, and Townsend DM (2010) Protective effects of a glutathione disulfide mimetic (NOV-002) against cisplatin induced kidney toxicity. *Biomedicine & pharmacotherapy = Biomedecine & pharmacotherapie* **64:**73-76.

Katsuda H, Yamashita M, Katsura H, Yu J, Waki Y, Nagata N, Sai Y, and Miyamoto K (2010) Protecting cisplatin-induced nephrotoxicity with cimetidine does not affect antitumor activity. *Biological & pharmaceutical bulletin* **33:**1867-1871.

Konig J, Muller F, and Fromm MF (2013) Transporters and drug-drug interactions: important determinants of drug disposition and effects. *Pharmacological reviews* **65:**944-966.

Konig J, Zolk O, Singer K, Hoffmann C, and Fromm MF (2011) Double-transfected MDCK cells expressing human OCT1/MATE1 or OCT2/MATE1: determinants of uptake and transcellular translocation of organic cations. *British journal of pharmacology* **163:**546-555.

Lash LH, Lee CA, Wilker C, and Shah V (2018) Transporter-dependent cytotoxicity of antiviral drugs in primary cultures of human proximal tubular cells. *Toxicology* **404-405:**10-24.

Lash LH, Putt DA, and Cai H (2006) Membrane transport function in primary cultures of human proximal tubular cells. *Toxicology* **228:**200-218.

Lash LH, Putt DA, and Cai H (2008) Drug metabolism enzyme expression and activity in primary cultures of human proximal tubular cells. *Toxicology* **244:**56-65.

Li Q, Guo D, Dong Z, Zhang W, Zhang L, Huang SM, Polli JE, and Shu Y (2013) Ondansetron can enhance cisplatin-induced nephrotoxicity via inhibition of multiple toxin and extrusion proteins (MATEs). *Toxicology and applied pharmacology* **273:**100-109.

Maass C, Sorensen NB, Himmelfarb J, Kelly EJ, Stokes CL, and Cirit M (2019) Translational Assessment of Drug-Induced Proximal Tubule Injury Using a Kidney Microphysiological System. *CPT: pharmacometrics & systems pharmacology* **8:**316-325.

Nakamura T, Yonezawa A, Hashimoto S, Katsura T, and Inui K (2010) Disruption of multidrug and toxin extrusion MATE1 potentiates cisplatin-induced nephrotoxicity. *Biochemical pharmacology* **80:**1762-1767.

Nielsen R, Christensen EI, and Birn H (2016) Megalin and cubilin in proximal tubule protein reabsorption: from experimental models to human disease. *Kidney international* **89:**58-67.

Nieskens TTG and Sjogren AK (2019) Emerging In Vitro Systems to Screen and Predict Drug-Induced Kidney Toxicity. *Seminars in nephrology* **39:**215-226.

Nigam SK, Wu W, Bush KT, Hoenig MP, Blantz RC, and Bhatnagar V (2015) Handling of Drugs, Metabolites, and Uremic Toxins by Kidney Proximal Tubule Drug Transporters. *Clinical journal of the American Society of Nephrology : CJASN* **10:**2039-2049.

Okuda M, Tsuda K, Masaki K, Hashimoto Y, and Inui K (1999a) Cisplatin-induced toxicity in LLC-PK1 kidney epithelial cells: role of basolateral membrane transport. *Toxicology letters* **106:**229-235.

Okuda M, Urakami Y, Saito H, and Inui K (1999b) Molecular mechanisms of organic cation transport in OCT2-expressing Xenopus oocytes. *Biochimica et biophysica acta* **1417:**224-231.

Pabla N, Murphy RF, Liu K, and Dong Z (2009) The copper transporter Ctr1 contributes to cisplatin uptake by renal tubular cells during cisplatin nephrotoxicity. *American journal of physiology Renal physiology* **296:**F505-511.

Petrillo M, Zucchetti M, Cianci S, Morosi L, Ronsini C, Colombo A, D'Incalci M, Scambia G, and Fagotti A (2019) Pharmacokinetics of cisplatin during open and minimally-invasive secondary cytoreductive surgery plus HIPEC in women with platinum-sensitive recurrent ovarian cancer: a prospective study. *Journal of gynecologic oncology* **30:**e59.

Raghavan V, Rbaibi Y, Pastor-Soler NM, Carattino MD, and Weisz OA (2014) Shear stress-dependent regulation of apical endocytosis in renal proximal tubule cells mediated by primary cilia. *Proceedings of the National Academy of Sciences of the United States of America* **111:**8506-8511.

Sakolish C, Weber EJ, Kelly EJ, Himmelfarb J, Mouneimne R, Grimm FA, House JS, Wade T, Han A, Chiu WA, and Rusyn I (2018) Technology Transfer of the Microphysiological Systems: A Case Study of the Human Proximal Tubule Tissue Chip. *Scientific reports* **8:**14882.

Sato T, Masuda S, Yonezawa A, Tanihara Y, Katsura T, and Inui K (2008) Transcellular transport of organic cations in double-transfected MDCK cells expressing human organic cation transporters hOCT1/hMATE1 and hOCT2/hMATE1. *Biochemical pharmacology* **76:**894-903.

Schmidt EK, Antonin KH, Flesch G, and Racine-Poon A (1998) An interaction study with cimetidine and the new angiotensin II antagonist valsartan. *European journal of clinical pharmacology* **53:**451-458.

Stahl S, Nordell P, Nieskens T, Fenner KS, and Caetano-Pinto P (2020) P245 - Investigation of renal drug secretion in a kidney-on-a-chip model. *Drug Metabolism and Pharmacokinetics* **35:**S97.

Stoops EH and Caplan MJ (2014) Trafficking to the apical and basolateral membranes in polarized epithelial cells. *Journal of the American Society of Nephrology : JASN* **25:**1375-1386.

Suter-Dick L, Mauch L, Ramp D, Caj M, Vormann MK, Hutter S, Lanz HL, Vriend J, Masereeuw R, and Wilmer MJ (2018) Combining Extracellular miRNA Determination with Microfluidic 3D Cell Cultures for the Assessment of Nephrotoxicity: a Proof of Concept Study. *The AAPS journal* **20:**86.

Townsend DM and Hanigan MH (2002) Inhibition of gamma-glutamyl transpeptidase or cysteine S-conjugate beta-lyase activity blocks the nephrotoxicity of cisplatin in mice. *The Journal of pharmacology and experimental therapeutics* **300:**142-148.

Townsend DM, Tew KD, He L, King JB, and Hanigan MH (2009) Role of glutathione S-transferase Pi in cisplatin-induced nephrotoxicity. *Biomedicine & pharmacotherapy = Biomedecine & pharmacotherapie* **63:**79-85.

Tsuda M, Terada T, Asaka J, Ueba M, Katsura T, and Inui K (2007) Oppositely directed H+ gradient functions as a driving force of rat H+/organic cation antiporter MATE1. *American journal of physiology Renal physiology* **292:**F593-598.

van der Made TK, Fedecostante M, Scotcher D, Rostami-Hodjegan A, Sastre Torano J, Middel I, Koster AS, Gerritsen KG, Jankowski V, Jankowski J, Hoenderop JGJ, Masereeuw R, and Galetin A (2019) Quantitative Translation of Microfluidic Transporter in Vitro Data to in Vivo Reveals Impaired Albumin-Facilitated Indoxyl Sulfate Secretion in Chronic Kidney Disease. *Molecular pharmaceutics* **16:**4551-4562.

Weber EJ, Chapron A, Chapron BD, Voellinger JL, Lidberg KA, Yeung CK, Wang Z, Yamaura Y, Hailey DW, Neumann T, Shen DD, Thummel KE, Muczynski KA, Himmelfarb J, and Kelly EJ (2016) Development of a microphysiological model of human kidney proximal tubule function. *Kidney international* **90:**627-637.

Weber EJ, Lidberg KA, Wang L, Bammler TK, MacDonald JW, Li MJ, Redhair M, Atkins WM, Tran C, Hines KM, Herron J, Xu L, Monteiro MB, Ramm S, Vaidya V, Vaara M, Vaara T, Himmelfarb J, and Kelly EJ (2018) Human kidney on a chip assessment of polymyxin antibiotic nephrotoxicity. *JCI insight* **3**.

Vedula EM, Alonso JL, Arnaout MA, and Charest JL (2017) A microfluidic renal proximal tubule with active reabsorptive function. *PloS one* **12:**e0184330.

Wittwer MB, Zur AA, Khuri N, Kido Y, Kosaka A, Zhang X, Morrissey KM, Sali A, Huang Y, and Giacomini KM (2013) Discovery of potent, selective multidrug and toxin extrusion transporter 1 (MATE1, SLC47A1) inhibitors through prescription drug profiling and computational modeling. *Journal of medicinal chemistry* **56:**781-795.

Vormann MK, Gijzen L, Hutter S, Boot L, Nicolas A, van den Heuvel A, Vriend J, Ng CP, Nieskens TTG, van Duinen V, de Wagenaar B, Masereeuw R, Suter-Dick L, Trietsch SJ, Wilmer M, Joore J, Vulto P, and Lanz HL (2018) Nephrotoxicity and Kidney Transport Assessment on 3D Perfused Proximal Tubules. *The AAPS journal* **20:**90.

Vriend J, Nieskens TTG, Vormann MK, van den Berge BT, van den Heuvel A, Russel FGM, Suter-Dick L, Lanz HL, Vulto P, Masereeuw R, and Wilmer MJ (2018) Screening of Drug-Transporter Interactions in a 3D Microfluidic Renal Proximal Tubule on a Chip. *The AAPS journal* **20:**87.

Yonezawa A, Masuda S, Nishihara K, Yano I, Katsura T, and Inui K (2005) Association between tubular toxicity of cisplatin and expression of organic cation transporter rOCT2 (Slc22a2) in the rat. *Biochemical pharmacology* **70:**1823-1831.

Yonezawa A, Masuda S, Yokoo S, Katsura T, and Inui K (2006) Cisplatin and oxaliplatin, but not carboplatin and nedaplatin, are substrates for human organic cation transporters (SLC22A1-3 and multidrug and toxin extrusion family). *The Journal of pharmacology and experimental therapeutics* **319:**879-886.

DMD Fast Forward. Published on October 5, 2020 as DOI: 10.1124/dmd.120.000098
This article has not been copyedited and formatted. The final version may differ from this version.

12. Footnotes

a) Tom Nieskens, Mikael Persson and Anna-Karin Sjögren are employees of AstraZeneca AB, Gothenburg, Sweden. Tom Nieskens is a fellow of the AstraZeneca Postdoc Programme.

b) Citation of meeting abstracts where the work was previously presented

1) Tom T.G. Nieskens and Anna-Karin Sjögren; A functionally polarized human kidney proximal tubule-on-a-chip for advanced drug-induced nephrotoxicity studies, Winter-meeting in the Danish Society for Pharmacology and Toxicology, 02-12-2019, Copenhagen, Denmark

c) Reprint requests can be directed to

Anna-Karin Sjögren

AstraZeneca R&D Mölndal

Pepparedsleden 1

43150 Mölndal

Sweden

anna-karin.sjogren@astrazeneca.com

d) This work was supported in part by the AstraZeneca Postdoc Programme.

e) Numbered footnotes

[1]CVRM Safety, Clinical Pharmacology and Safety Sciences, AstraZeneca, Gothenburg, Sweden

[2]Department of Pharmaceutics, University of Washington, Seattle, USA

[3]Kidney Research Institute, University of Washington, Seattle, USA

DMD Fast Forward. Published on October 5, 2020 as DOI: 10.1124/dmd.120.000098
This article has not been copyedited and formatted. The final version may differ from this version.

13. Legends for Figures

Figure 1: Characterization of the polarized human-derived kidney proximal tubule-on-a-chip. (A) Layout of the Nortis® dual channel chip with the extracellular matrix compartment (ECM, red) which contains 2 hollow channels (black box) that are coupled to an independent PDMS perfusion circuit (blue), which are in turn fed by medium reservoirs located at the inflow positions. Courtesy of Nortis, Inc. (B) Phase contrast image shows that a 3D HRPTEC tube is formed inside the hollow channel after injection and medium perfusion for 7 days, with a distinct luminal compartment, forming the apical channel, while the parallel basolateral channel is only perfused with medium (original magnification 4x). (C) Immunofluorescent confocal image shows a typical epithelial localization pattern of tight junction protein (ZO-1, *TJP1*) at the interface between HRPTEC and positive staining for HRPTEC marker Lotus Lectin (LTL); both correctly localized at the apical brush border membrane on the luminal side of the tube. Phalloidin stained for F-actin that outlines the borders of HRPTEC and OCT2 (*SLC22A2*) is strictly localized on the basolateral membrane on the ECM side of the tube. Staining for acetylated alpha tubulin demonstrates the presence of primary cilia, protruding from the apical membrane into the tubule lumen, confirming epithelial polarization of HRPTEC in the proximal tubule-on-a-chip. (D) 3D projection (30 degrees) of 60 confocal microscopy planes demonstrate the continuity of tight junction protein (ZO-1) immunofluorescent staining throughout the HRPTEC tube. (E) Cut-through overview of the proximal tubule-on-a-chip and imaging positions used for confocal microscopy.

Figure 2: Gene expression levels in human-derived kidney proximal tubule cells cultured in the chip compared to regular 2D cultures. Gene expression analysis of drug transporters, endocytosis receptors and PTEC markers show a significantly higher MATE1 (*SLC47A1*), MATE2-k (*SLC47A2*), BCRP (*ABCG2*) and Megalin endocytosis receptor (*LRP2*) gene expression in HRPTEC cells cultured for 7 days in chips compared to HRPTEC cells cultured for the same time in 2D, while expression of P-gp (*ABCB1*) is reduced, using *GAPDH* as reference gene (mean±S.D., gene expression in chip-cultured HRPTEC compared with 2D cultures by multiple Student's t tests, n=5 (number of biological replicates set in advance except otherwise indicated); n=8 (*GAPDH*; due to inclusion of additional biological replicates

DMD Fast Forward. Published on October 5, 2020 as DOI: 10.1124/dmd.120.000098
This article has not been copyedited and formatted. The final version may differ from this version.

after experimental design); n=4 (*AQP1*; due to technical error); n=3 (*ABCG2, SLC5A2, SLC22A1, SLC22A4, SLC22A5, SLC31A1, SLCO4C1*; due to inclusion after experimental design), performed with 1 experimental replicate, 18 comparisons in total, **P<0.01; ***P<0.001; ****P<0.0001 (corrected for multiple comparisons using the Holm-Sidak method)).

Figure 3: Transepithelial transfer of fluorescent organic cation 4-di-1-ASP in the proximal tubule-on-a-chip. (A) Fluorescent cation 4-di-1-ASP (100 µM) was perfused at 2 µl/min into the basolateral compartment of the proximal tubule-on-a-chip, with or without competitive OCT2 inhibitor cimetidine (1 mM), while HBSS-HEPES buffer was perfused into the apical compartment. (B) Fluorescence intensity of 4-di-1-ASP in accumulative apical perfusate (8612±5208) was not significantly reduced (P=0.18) upon co-incubation with cimetidine (1 mM) (4956±3616, mean±S.D., fluorescence intensity of the apical perfusate without cimetidine compared to with cimetidine by paired Student's t test, n=3 (with the number of biological replicates set in advance), performed with 1 experimental replicate, 1 comparison in total).

Figure 4: Membrane-dependent cisplatin-induced toxicity in the human-derived kidney proximal tubule-on-a-chip. Cisplatin (25 µM, 72 h) induced toxicity when perfused from the basolateral compartment, but not the apical compartment, and is abolished by co-perfusion with OCT2 inhibitor cimetidine (1 mM) as evaluated by (A) Disruption of tight junctions at the bottom and middle planes of chip-cultured HRPTEC, (B) Reduced nuclei count and (C) Reduced epithelial barrier integrity according to the figure in (D). Analysis of (A) (n=5 (vehicle; 25 µM basolateral; 25 µM apical) and n=4 (25 µM basolateral, cimetidine) with all biological replicates set in advance, performed with 1 experimental replicate, representative images were selected, original magnification 20x). (B) (mean±S.D., Hoechst count in the 'bottom' images compared to vehicle by one-way ANOVA with Dunnett's multiple comparisons test, n=5 (vehicle; 25 µM basolateral; 25 µM apical) and n=4 (25 µM basolateral, cimetidine) with all biological replicates set in advance, performed with 1 experimental replicate, 3 comparisons in total, ****P<0.0001 (multiplicity adjusted P values)). (C) (mean±S.D., dextran 3000-Alexa Fluor 680 fluorescence intensity sampled from the basolateral channel perfusate compared to time-matched vehicle by two-way ANOVA with Dunnett's multiple comparisons test, n=4 (vehicle; 25 µM basolateral; 25 µM

DMD Fast Forward. Published on October 5, 2020 as DOI: 10.1124/dmd.120.000098
This article has not been copyedited and formatted. The final version may differ from this version.

apical) and n=3 (25 µM basolateral, cimetidine) with 1 biological replicate excluded due to technical error, performed with 1 experimental replicate, 12 comparisons in total, ****P<0.0001 (multiplicity adjusted P values)). Cim: supplemented with cimetidine (1 mM).

Figure 5: Differences in exposure of the HPRTEC channel depending on basolateral or apical perfusion of cisplatin. (A) Basolateral perfusion aims to mimic clinically-relevant exposure by perfusing cisplatin into the basolateral (parallel) channel, followed by diffusion through the collagen I matrix, resulting in exclusive exposure of the HRPTEC basolateral membrane (B) Apical perfusion of cisplatin directly in the apical HRPTEC channel (C) Cisplatin concentration in the HRPTEC channel is significantly reduced when cisplatin (25 µM) is perfused through the basolateral compartment compared to the apical compartment as indicated in (A) and (B) taking non-accumulating samples every 12 h for 72 h (mean±S.D., basolateral concentration compared to time-matched apical concentration by multiple Student's t tests, n=4 (12, 36-72 h) and n=3 (24 h) with 1 biological replicate at 24 h excluded due to technical error, performed with 1 experimental replicate, 6 comparisons in total, ****P<0.0001 (corrected for multiple comparisons using the Holm-Sidak method)).

DMD Fast Forward. Published on October 5, 2020 as DOI: 10.1124/dmd.120.000098
This article has not been copyedited and formatted. The final version may differ from this version.

14. Tables

Table 1: Gene expression levels of drug transporters, endocytosis receptors, tight junction protein and proximal tubule markers in regular 2D cultures and Nortis chip cultures of HRPTEC[a]

Gene	**Ct**		**-ΔΔCt**	
	2D HRPEC	**Nortis HRPTEC**	**2D HRPTEC**	**Nortis HRPTEC**
GAPDH	16.2 ± 1.1	17.4 ± 0.5		
HPRT1	20.9 ± 0.9	22.2 ± 0.5	0.0 ± 0.4	0.2 ± 0.6
ABCB1	19.9 ± 0.8	23.0 ± 0.4	0.0 ± 0.6	-1.7 ± 0.3
ABCC4	21.5 ± 0.9	23.1 ± 0.7	0.0 ± 0.4	-0.2 ± 0.7
ABCG2	34.5 ± 0.2	33.0 ± 0.4	0.0 ± 0.1	2.1 ± 0.1
SLC5A2	32.4 ± 0.2	32.3 ± 0.2	0.0 ± 0.3	0.6 ± 0.3
SLC22A1	31.4 ± 0.1	31.9 ± 0.3	0.0 ± 0.2	0.1 ± 0.2
SLC22A2	24.2 ± 0.5	25.1 ± 0.6	0.0 ± 0.9	0.5 ± 0.7
SLC22A4	28.5 ± 0.1	28.9 ± 0.4	0.0 ± 0.1	0.1 ± 0.1
SLC22A5	25.6 ± 0.1	26.4 ± 0.2	0.0 ± 0.1	-0.1 ± 0.1
SLC22A6	N.D[b]	29.0 ± 0.8		
SLC22A8	N.D[b]	N.D[b]		
SLC31A1	24.2 ± 0.1	24.6 ± 0.2	0.0 ± 0.1	0.3 ± 0.1
SLC47A1	31.0 ± 0.4	28.2 ± 0.4	0.0 ± 1.0	4.3 ± 0.4
SLC47A2	28.7 ± 1.5	25.7 ± 0.4	0.0 ± 1.8	4.5 ± 0.5
SLCO4C1	22.2 ± 0.1	22.9 ± 0.3	0.0 ± 0.1	-0.1 ±0.1
LRP2	34.0 ± 1.8	28.7 ± 0.5	0.0 ± 1.4	6.7 ± 0.4
CUBN	27.1 ± 0.7	27.9 ± 0.4	0.0 ± 0.5	0.6 ± 0.4
AQP1	23.1 ± 0.8	23.2 ± 0.7	0.0 ± 0.6	1.0 ± 0.7
TJP1	20.7 ± 0.9	21.8 ± 0.5	0.0 ± 0.3	-0.1 ± 0.2
GGT1	19.6 ± 1.8	19.7 ± 1.5	0.0 ± 1.1	0.7 ± 1.0

[a]mean ± SD; [b]Not Detected

DMD Fast Forward. Published on October 5, 2020 as DOI: 10.1124/dmd.120.000098
This article has not been copyedited and formatted. The final version may differ from this version.

15. Figures

Figures were uploaded separately.

Figure 1

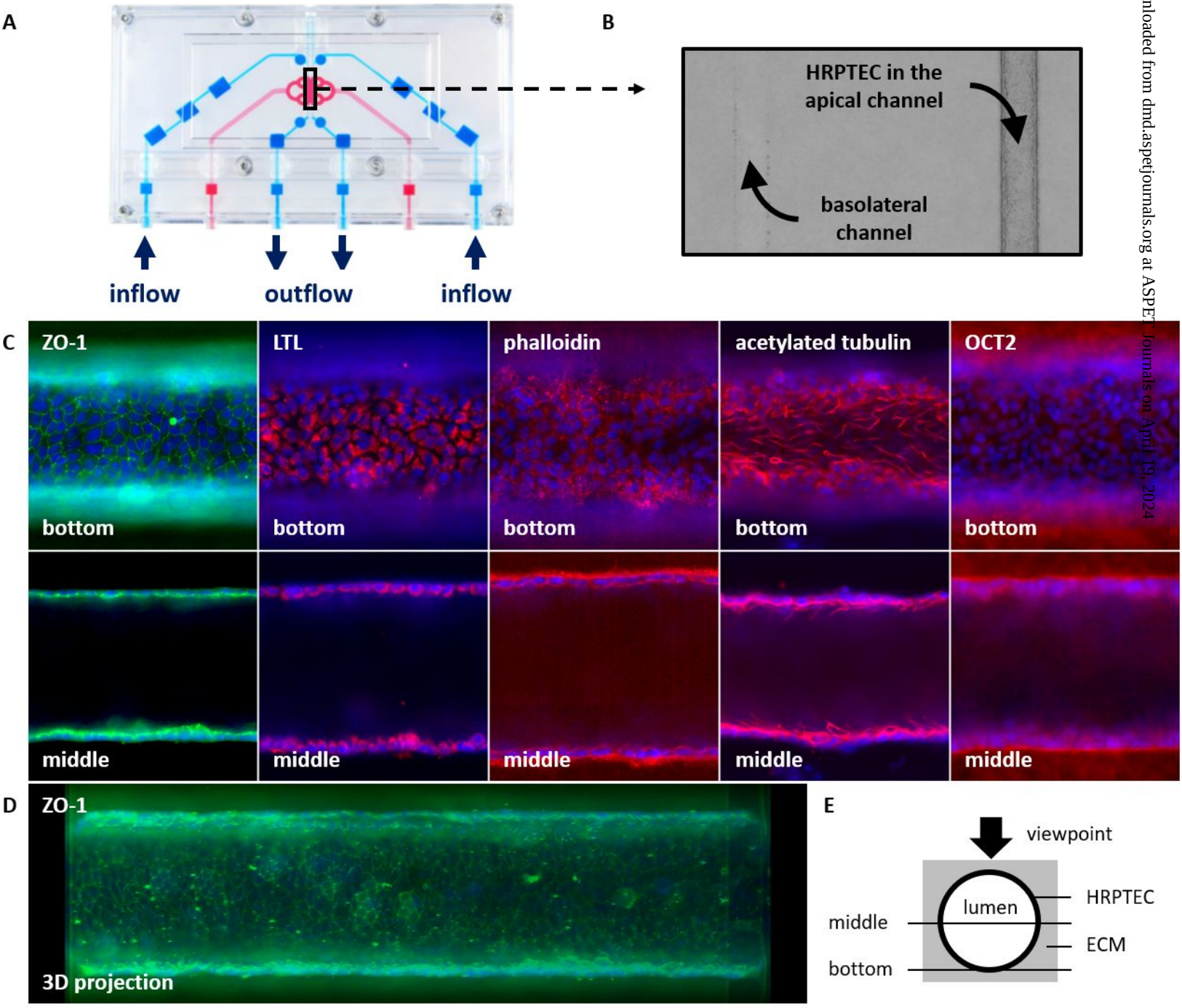

Figure 2

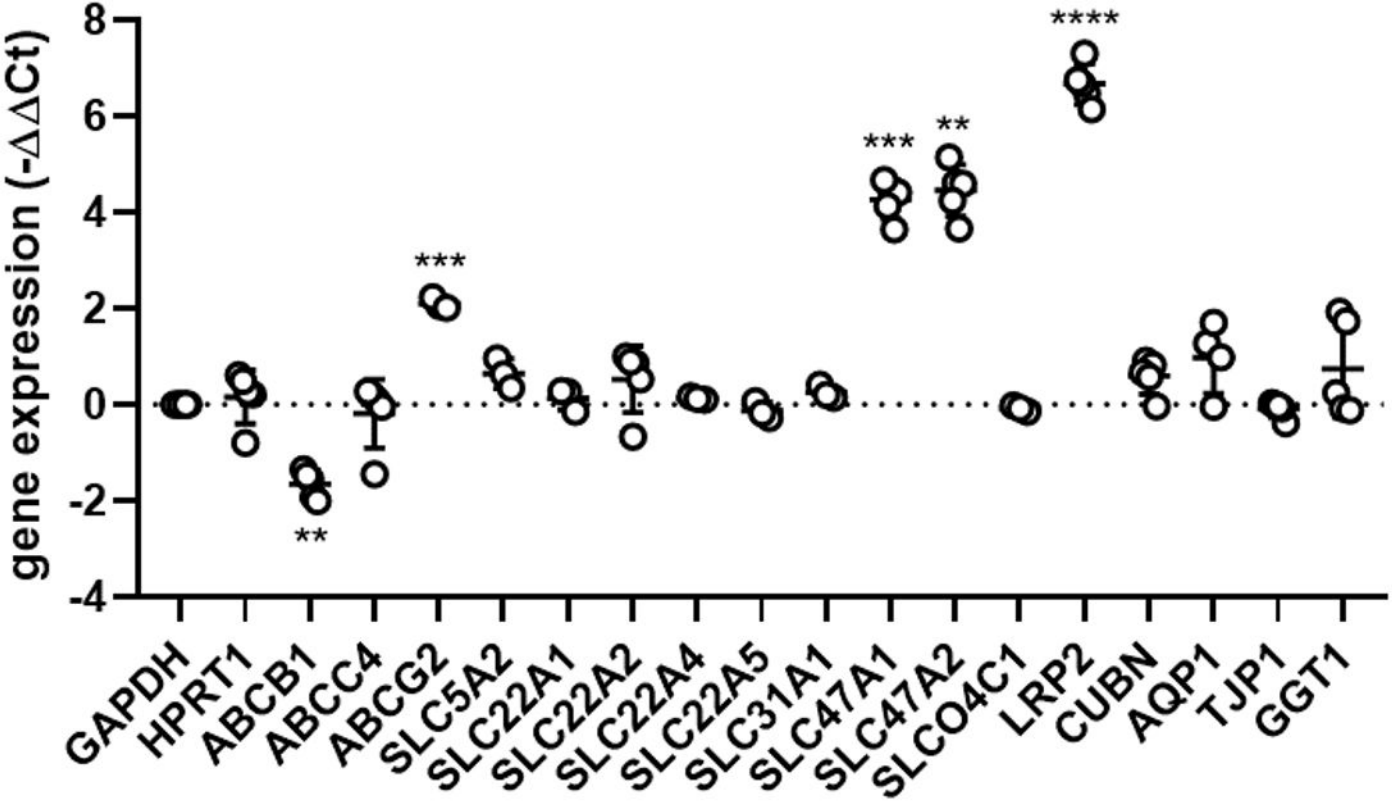
gene expression (-ΔΔCt)
8
6
4
2
0
-2
-4
**
***
***
**
****
GAPDH
HPRT1
ABCB1
ABCC4
ABCG2
SLC5A2
SLC22A1
SLC22A2
SLC22A4
SLC22A5
SLC31A1
SLC47A1
SLC47A2
SLCO4C1
LRP2
CUBN
AQP1
TJP1
GGT1

Figure 3

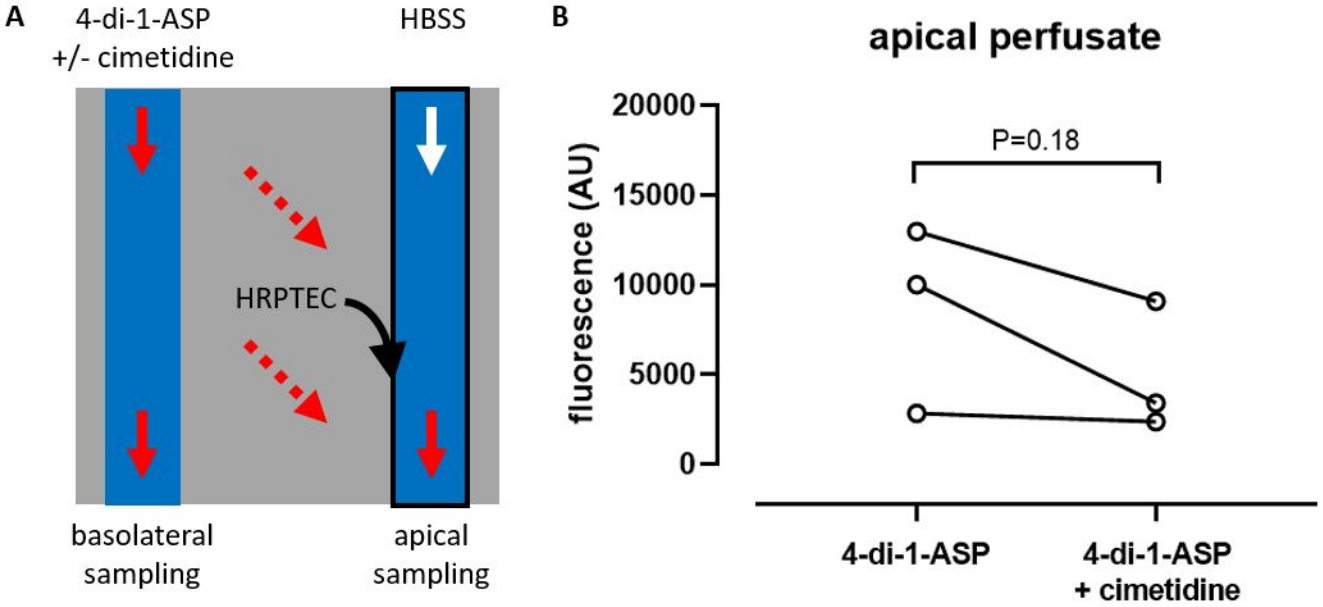
A
4-di-1-ASP
+/- cimetidine
HBSS
HRPTEC
basolateral
sampling
apical
sampling
B
apical perfusate
fluorescence (AU)
20000
15000
10000
5000
0
P=0.18
4-di-1-ASP
4-di-1-ASP
+ cimetidine

Figure 4

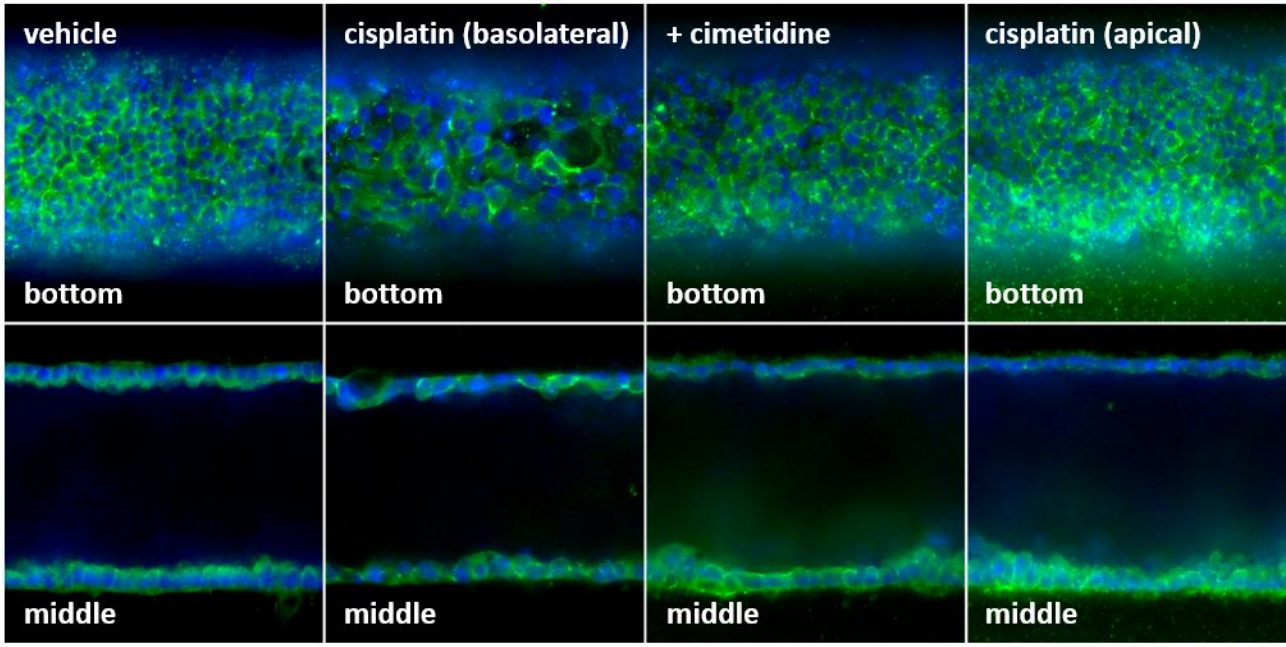
A
vehicle
cisplatin (basolateral)
+ cimetidine
cisplatin (apical)
bottom
bottom
bottom
bottom
middle
middle
middle
middle

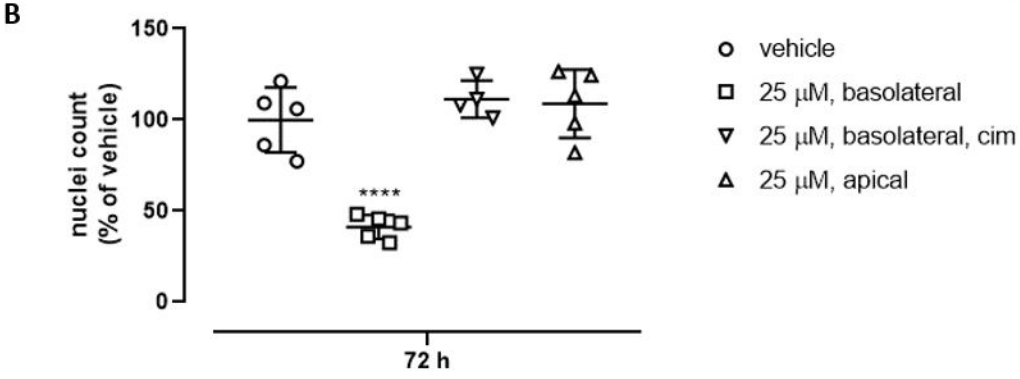
B
nuclei count (% of vehicle)
150
100
50
0
****
72 h
vehicle
25 µM, basolateral
25 µM, basolateral, cim
25 µM, apical

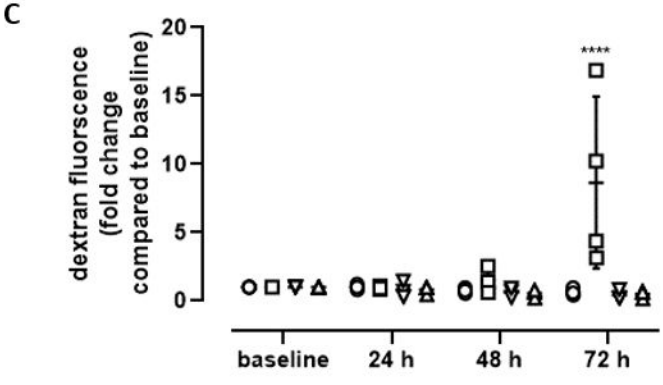
C
dextran fluorscence (fold change compared to baseline)
20
15
10
5
0
****
baseline
24 h
48 h
72 h

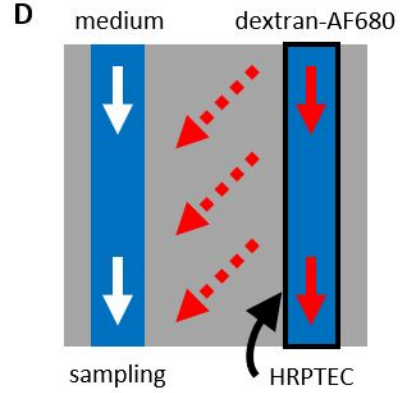
D
medium
dextran-AF680
sampling
HRPTEC

Figure 5

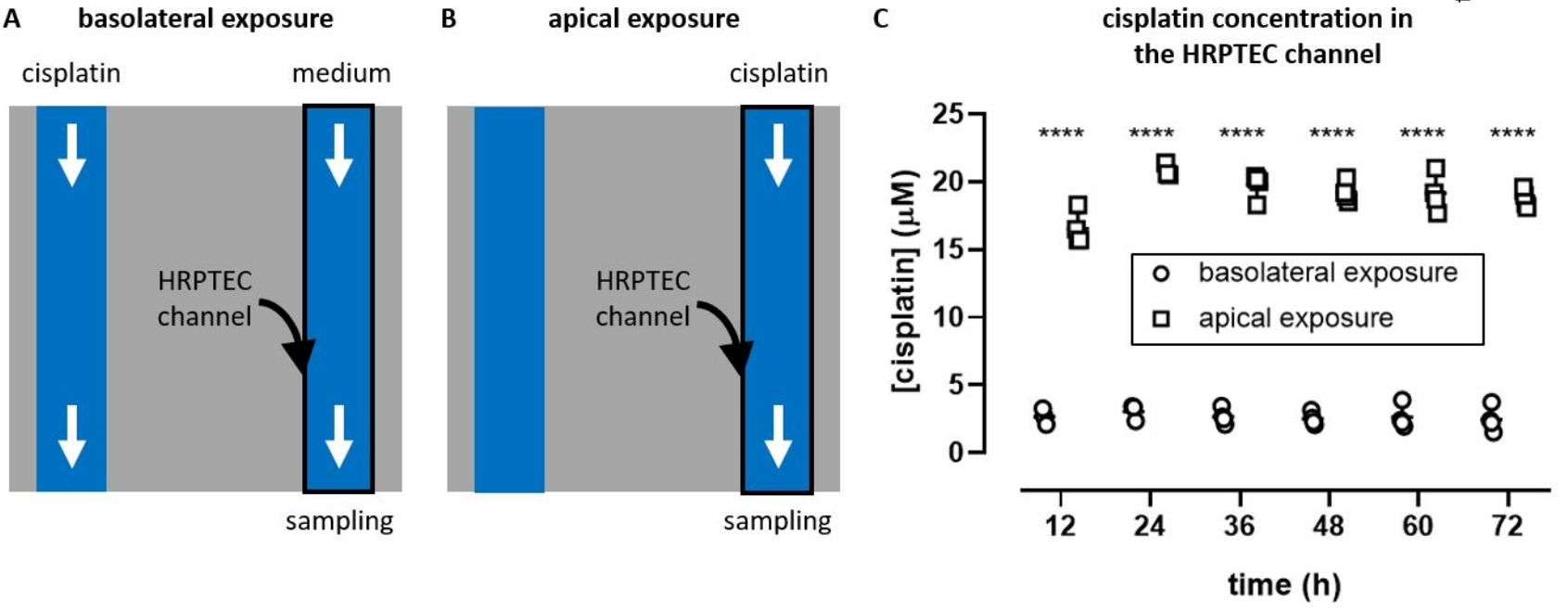
A
basolateral exposure
cisplatin
medium
HRPTEC
channel
sampling
B
apical exposure
cisplatin
HRPTEC
channel
sampling
C
cisplatin concentration in
the HRPTEC channel
[cisplatin] (μM)
25
20
15
10
5
0
****
basolateral exposure
apical exposure
12
24
36
48
60
72
time (h)